

## Precipitation-induced quenching of $\text{Eu}^{2+}$ luminescence in potassium halides

J. E. Muñoz Santiuste and J. García Solé

*Departamento de Física Aplicada C-IV, Universidad Autónoma de Madrid, Cantoblanco 28049, Madrid, Spain*

M. Manfredi

*Dipartimento di Fisica, Università di Parma, Gruppo Nazionale di Struttura della Materia, Consiglio Nazionale delle Ricerche, Viale della Scienze, 43100 Parma, Italy*

(Received 15 June 1990)

The effect of the  $\text{Eu}^{2+}$  precipitation state on the luminescence and decay time of europium-doped potassium halides has been systematically investigated. Each type of Eu precipitate is well characterized by a distinct lifetime. Nucleation of  $\text{EuX}_2$ -type precipitates ( $X=\text{Cl}, \text{Br}, \text{or I}$ ) strongly reduces the lifetime of  $\text{Eu}^{2+}$  as compared to the lifetime of quenched samples (which is on the order of  $1 \mu\text{s}$ ). This reduction can be explained by a concentration quenching of emitted light in these types of precipitates. On the other hand, nucleation of the other type of Eu precipitates (which have been previously tentatively associated with Suzuki phase structures) does not produce this quenching of light, and only a slight increase in their lifetime value, due to the new environment, is now observed.

### I. INTRODUCTION

Optical absorption and fluorescence spectra of the  $\text{Eu}^{2+}$  ion have been traditionally used<sup>1-6</sup> to analyze the europium precipitation processes in alkali halide crystals. This has been possible because of the sensitivity of the optical properties of this ion to its local environment. In fact, it is well known that each precipitation state is well characterized by a defined emission band.

On the other hand, recent experimental works<sup>7-11</sup> on the decay time scheme of  $\text{Eu}^{2+}$  luminescence in these materials have shown that lifetime measurements were also sensitive to the precipitation state. Taking advantage of this effect, it was shown that lifetime measurements could be used as an alternative technique to investigate precipitation process in europium-doped alkali halides.

In a recent paper<sup>12</sup> we reported a systematic investigation on the luminescence decay time associated with the evolution of the precipitation phenomena of  $\text{Eu}^{2+}$  in monocrystalline sodium chloride. It was found that the overall emitted light strongly decreased when the precipitation processes, leading to the formation of  $\text{EuCl}_2$ -type precipitates, took place. Thus the changes observed in the  $\text{Eu}^{2+}$  fluorescence lifetime were mainly due to a precipitation-induced quenching.

In this paper a systematic study of the evolution of the  $\text{Eu}^{2+}$  luminescence decay time, with several thermal treatments leading to different europium precipitation states, has been made for three potassium halide host matrices (KCl, KBr, and KI). In these systems, in addition to the heterogeneous dihalide-type phase, the formation of a secondary homogeneous phase can be induced by the use of suitable thermal treatments. These kinds of precipitates, which are optically well characterized, were tentatively associated with the so-called Suzuki phase particles, which are coherent with the host matrix and have stoichiometry  $6\text{KX}:\text{EuX}_2$  ( $X=\text{Cl}, \text{Br}, \text{or I}$ ), al-

though a final assignment via x-ray diffraction is not available for these  $\text{Eu}^{2+}$ -doped systems.

All experimental data reported in this work were obtained by exciting the samples with light of 337 nm ( $\text{N}_2$ -pulsed laser for decay time measurements and 150-W xenon lamp for continuous emission measurements) which lies in the  $\text{Eu}^{2+}$  low-energy absorption band. Other experimental details and data analysis are similar to those described in our previous paper.<sup>12</sup> Emission spectra presented in this work have been taken at room temperature to compare with previously reported experimental data.

### II. EXPERIMENTAL RESULTS

As previously reported,<sup>1-6</sup> the optical-absorption spectra of our  $\text{Eu}^{2+}$ -doped samples consist in two broad and structured bands, which are unequivocally associated to transitions from the  $4f^7(^8S_{7/2})$  ground state to the  $t_{2g}$  and  $e_g$  components of the  $4f^65d$  excited state. The position of the center of gravity of these broad bands depends on the host, as well as on the aggregation and precipitation state of europium ions. For a given europium dispersion state, the separation in energy between these broad bands allows the determination of the cubic crystal field,  $10Dq$ , acting on the  $\text{Eu}^{2+}$  site.

Excitation into the two absorption bands produced the same emission spectrum in all cases, although the efficiency was slightly decreased when excited in the high-energy band. This fact indicates multiphonon relaxation, from the high to the lower excited state component. The loss of efficiency can be understood in terms of the afterglow luminescence reported for  $\text{Eu}^{2+}$ -doped alkali halides under excitation with light lying into the high-energy absorption band.<sup>13</sup> As has been previously stated, in this work all experimental data were taken by exciting with light lying into the low-energy component.

Therefore, the afterglow luminescence, which could be masking our decay time plots, is not affecting our results.

It is well known that the final  $\text{Eu}^{2+}$ -type precipitate, which is formed after thermal annealing of europium-doped potassium halide crystals, is strongly dependent on the temperature of annealing. High-temperature annealing of quenched samples ( $T \geq 200^\circ\text{C}$ ) leads to the formation of the stable dihalide phase  $\text{EuX}_2$  ( $X=\text{Cl, Br, or I}$ ).<sup>2,4,6</sup> In order to reach this final prescription state, two intermediate metastable Eu precipitates (only one in the KBr system) are initially formed, which finally develop in the stable dihalide phase. On the other hand, annealing at moderately high temperatures ( $T \leq 100^\circ\text{C}$ ) produces the formation of other types of Eu precipitates, which have been initially related to a cubic Suzuki phase. Recent Raman spectroscopic results<sup>14</sup> do not support this assignment, but we will label it as a Suzuki-type phase, indicating that the nucleation of this phase is homogeneous with the crystal structure.<sup>15</sup> The above-mentioned Eu precipitates are well characterized by a defined emission band, whose maxima peak positions are shifted to longer wavelengths, and bigger  $10Dq$  values, than those obtained for the quenched samples.

According to our previous comments, the experimental results obtained in this work have been separately presented, depending on the temperature range of annealing.

#### A. High-temperature-annealed samples ( $T \geq 200^\circ\text{C}$ )

Figure 1(a) shows the emission spectra for  $\text{Eu}^{2+}$ -doped KCl, KBr, and KI crystals annealed at temperatures in the range  $200\text{--}300^\circ\text{C}$ . Each one of the spectra is composed of the same Gaussian overlapping bands that have been previously reported for samples nucleating  $\text{EuX}_2$  precipitates ( $X=\text{Cl, Br, or I}$ ). The peak position of the different emission bands have been included in Table I, together with the corresponding Eu precipitate. The emission band correlated with the Eu-dissolved impurity (impurity-vacancy dipoles and small aggregates) appears in all cases, and it is the only one remaining after quenching the sample from  $500^\circ\text{C}$ .

The cubic crystal field acting on the impurity site in each dispersion state (precipitated or dissolved) can be calculated from the excitation spectra of the different emission bands. It has been measured as the  $10Dq$  splitting, and it is also included in Table I. The values obtained are in good agreement with those formerly reported for the different dihalide phases, as precipitated in the same alkali halides. This fact indicates that the same type of europium precipitates are now formed.

The fluorescence decay time has been studied in parallel to the continuous emission measurements during the thermal annealing treatments leading to the precipitation states defined by the spectra of Fig. 1(a). This study, ex-

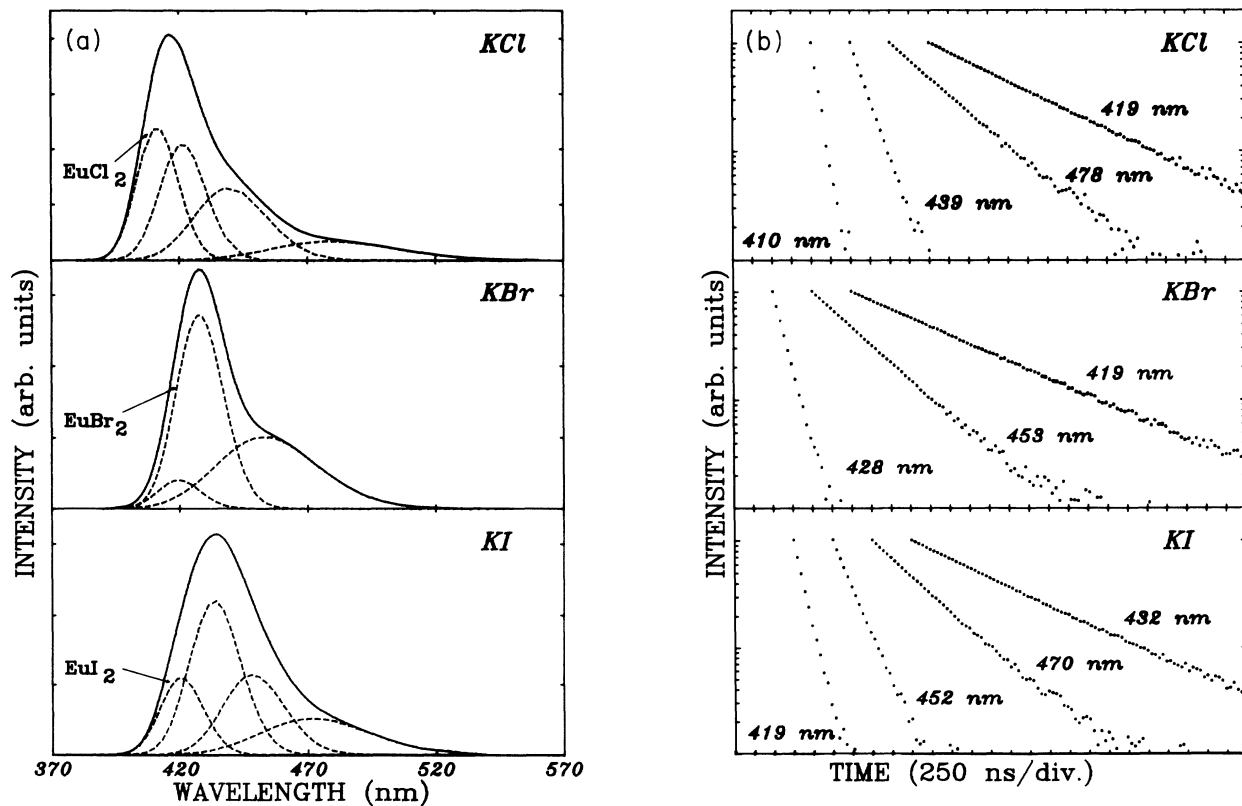


FIG. 1. (a) Room-temperature emission spectrum of  $\text{Eu}^{2+}$ -doped KCl, KBr, and KI samples annealed, respectively, during 600, 240, and 470 h at  $220^\circ\text{C}$  ( $\lambda_{\text{exc}} = 337 \text{ nm}$ ). (b) Decay time plots of the different emission bands.

TABLE I. Spectroscopic parameters for the different Eu precipitates appeared in high-temperature-annealed samples ( $T \geq 200^\circ\text{C}$ ). Stable dihalide phase and quenched samples are indicated. Other peak wavelengths correspond to intermediate Eu phases.

Host	Peak position of emission band (nm)	$10Dq$ ( $\text{cm}^{-1}$ )	Lifetime ( $\mu\text{s}$ )	Overlap $\Omega$ ( $E = eV$ )	Critical distance $R_c$ ( $\text{\AA}$ )
KCl	410 $\text{EuCl}_2$	9743	0.09	$2.27 \times 10^{-4}$	16.7
	439	9369	0.20	$2.03 \times 10^{-5}$	10.8
	478	9677	0.67	$8.87 \times 10^{-7}$	6.4
	419 quenched	12 167	1.20		
KBr	428 $\text{EuBr}_2$	9434	0.15	$3.13 \times 10^{-4}$	12.6
	453	9174	0.65	$6.23 \times 10^{-5}$	9.6
	419 quenched	10 749	1.23		
KI	419 $\text{EuI}_2$	9121	0.13	$6.57 \times 10^{-4}$	15.6
	452	8823	0.24	$5.03 \times 10^{-5}$	10.2
	470	9044	0.64	$1.34 \times 10^{-5}$	8.2
	432 quenched	9808	1.33		

tended to different emission wavelength, shows that each emission band is associated with a single exponential decay, but, due to overlapping between them, the fluorescence decay time curves usually appear as nonexponential ones. In Fig. 1(b), the resolved fluorescence decay time plots, corresponding to each emission band, have been displayed for the different systems investigated in this work. An inspection of this figure reveals that the lifetime of precipitates are reduced if they are compared with the values corresponding to freshly quenched samples associated to the dissolved impurity (which are on the order of  $1 \mu\text{s}$ ). The reduction is higher in the case of the stable  $\text{EuX}_2$  particles formed in the three investigated potassium halides. A very similar behavior was found for these precipitates when they were embedded in NaCl (Ref. 12), and it was explained as a consequence of a precipitation-induced quenching of the  $\text{Eu}^{2+}$  luminescence in these particles. This fact was due to the proximity between divalent ions when the stable dihalide phase was nucleated. Consequently, the same kind of mechanism should be taking place now.

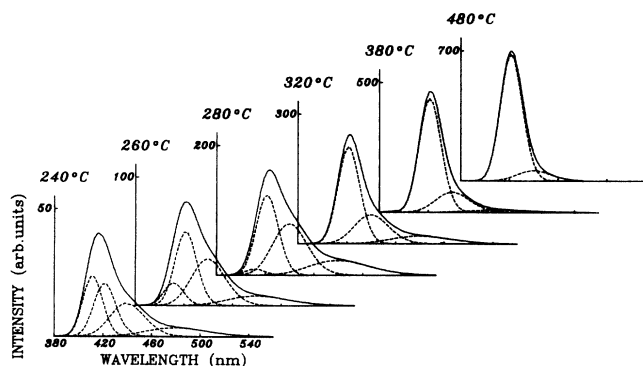


FIG. 2. Evolution of the emission spectrum vs quenching temperature for the  $\text{KCl}:\text{Eu}^{2+}$  sample of Fig. 1(a). (Note the different scales for the light intensity axis.)

In order to ascertain this mechanism in the potassium halides here investigated, the overall emitting light was measured as a function of the europium precipitation state. This experiment becomes necessary for checking the existence of nonradiative decay channels, which can explain the experimental reduction observed in the life-

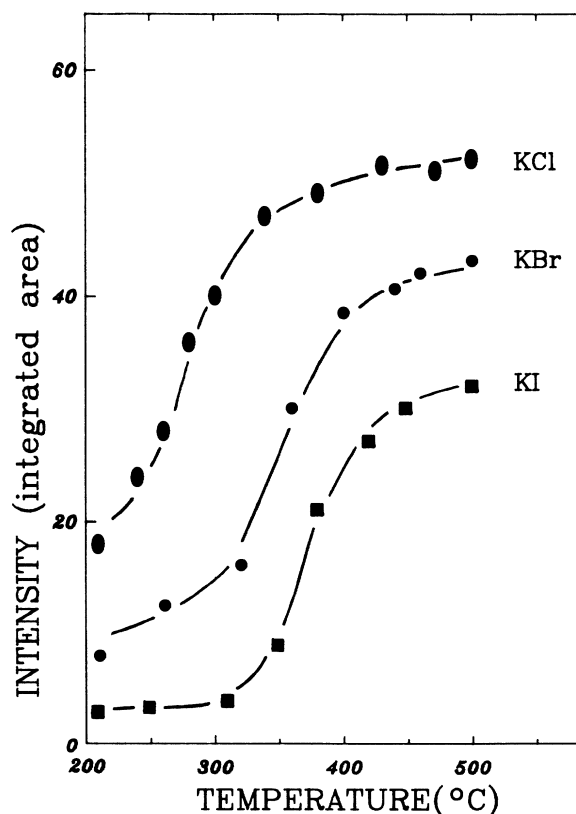


FIG. 3. Emission intensity (area under the curve) as a function of quenching temperature for precipitated phases formed under annealing at  $T \geq 200^\circ\text{C}$  for the three systems investigated in this work.

TABLE II. Spectroscopic parameters for the different Eu precipitates appeared in low-temperature-annealed samples ( $T \leq 100^\circ\text{C}$ ).

Host	Peak position of emission band (nm)	$10Dq$ ( $\text{cm}^{-1}$ )	Lifetime ( $\mu\text{s}$ )	Overlap $\Omega$ ( $E = eV$ )	Critical distance $R_c$ ( $\text{\AA}$ )
KCl	429	12 647	1.34	$4.50 \times 10^{-6}$	6.27
KBr	432	11 512	1.86	$7.69 \times 10^{-6}$	7.09
KI	440	10 167	1.64	$1.91 \times 10^{-5}$	8.81

time. To perform these measurements, the same precipitated samples of Fig. 1(a) were heated up to a given temperature, kept at this temperature for 10 min, and then quenched down to room temperature to take the optical measurements. This procedure was reported systematically for increasing temperatures. Figure 2 shows, as an example, the evolution of emission spectra versus temperature of annealing treatments for the KCl system. Thermal dissolution of the precipitates and the disappearance of their associated emission bands (479 and 439 nm) are taking place in the temperature range of 200–500 °C. At the same time, the 419-nm band, responsible for the dissolved impurity, is growing, being the only one remaining after quenching at 500 °C. It is important to point out that the overall emitted light increases with quenching temperature, when the dissolu-

tion of precipitated phases is taking place (note the different scale in the intensity axis). This fact can be clearly appreciated in Fig. 3, in which the total emission intensity (area under the emission spectrum) has been displayed as a function of annealing temperature for the three systems investigated in this work. This result clearly shows that quenching of  $\text{Eu}^{2+}$  emitted light occurs during precipitation. Furthermore, this precipitation-induced quenching of light is not thermally activated, because the area under the emission spectra for a given precipitation state is decreasing only slightly with an increase of the temperature from 10 to 300 K.

On the other hand, the lifetime of each fluorescence band remained constant (within experimental error) during either the dissolution thermal treatment or the annealing treatment, leading to the final precipitation state

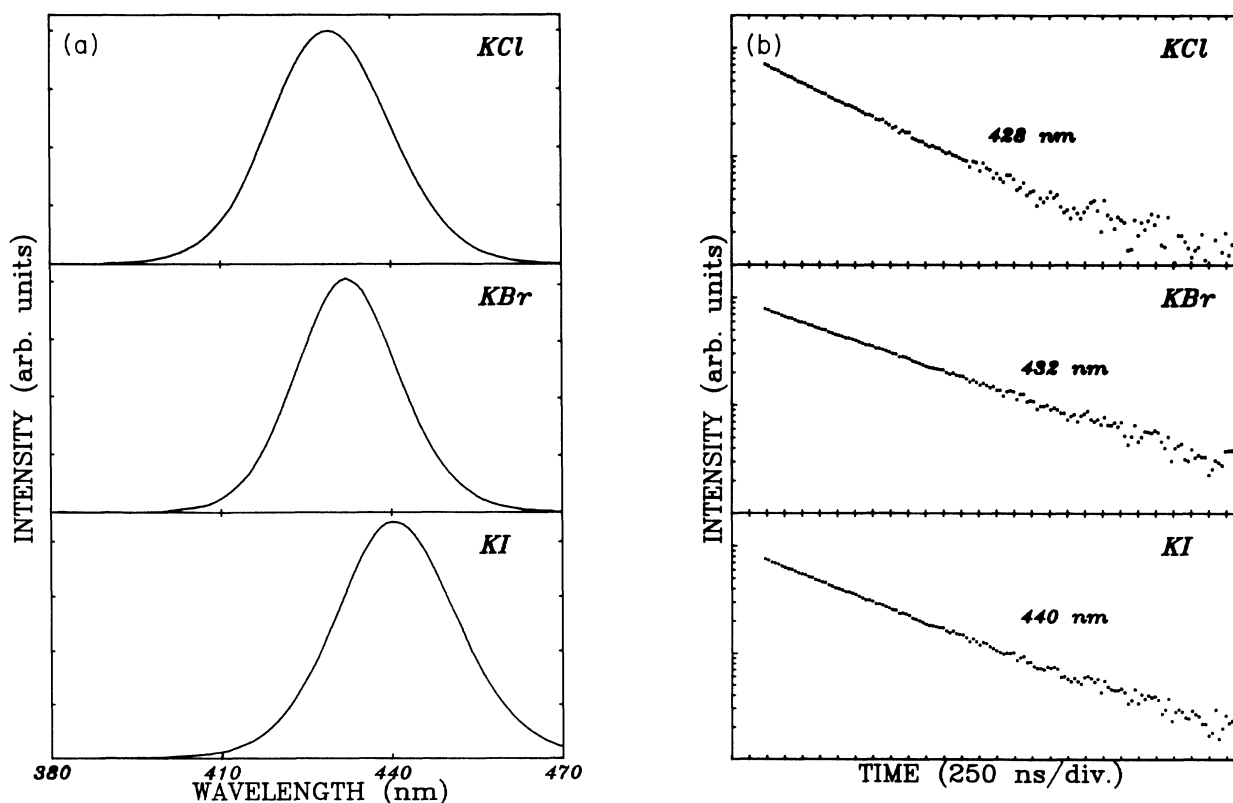


FIG. 4. (a) Room-temperature emission spectrum of  $\text{Eu}^{2+}$ -doped KCl, KBr, and KI samples annealed, respectively, during 560, 740 and 1140 h at  $80^\circ\text{C}$  ( $\lambda_{\text{exc}} = 337 \text{ nm}$ ). (b) Decay time plots of these emission bands.

of Fig. 1. This fact indicates that the lifetimes probably remain constant with the size of the various europium precipitates.

### B. Moderately high-temperature-annealed samples ( $T \leq 100^\circ\text{C}$ )

By annealing the samples at temperatures below  $100^\circ\text{C}$ , the emission spectra, and consequently the corresponding Eu precipitates, are different from those observed in Sec. II A. Figure 4(a) shows the emission spectra for KCl, KI, and KBr europium-doped samples annealed during long times at temperatures between  $100^\circ\text{C}$ . The emission spectrum of each sample consists now of one band which is shifted to lower energies, as compared with the emission of the quenched samples. These bands have been previously reported for the same kind of crystals, and were tentatively reported as Suzuki phase precipitates. Peak positions, as well as  $10Dq$  crystal-field values (slightly higher than those found for quenched samples), are included in Table II. These results are also in good agreement with previously reported data,<sup>1,4,6</sup> and therefore the same kind of precipitates are nucleating in our crystals.

Taking advantage of the very simple emission spectrum observed now, decay time analyses were very easy.

At variance with the high-temperature-annealed samples (Sec. II A), the Eu precipitates, which are now developing, show a single exponential decay [see Fig. 4(b)] with a lifetime slightly higher than those of quenched samples. The greatest difference is found in the KBr system.

Therefore, precipitation-induced quenching should not be taking place for these Eu precipitates. This fact is evidenced in Fig. 5, where it is shown that the total intensity of the emission spectrum of each system remains constant during the thermal dissolution of the Suzuki precipitates, which takes place at temperatures  $\leq 250^\circ\text{C}$ .<sup>1,4,6</sup>

### III. DISCUSSION

In a way similar to the  $\text{NaCl}:\text{Eu}^{2+}$  system, the reduction of the  $\text{Eu}^{2+}$  emission lifetime value can be explained by a concentration quenching of emitted light, induced by europium precipitation, followed by some kind of radiationless channel.

Obviously, precipitation phenomena reduce the  $\text{Eu}^{2+}$ - $\text{Eu}^{2+}$  distance, and therefore energy migration along the precipitate can take place.  $\text{Eu}^{2+}$ - $\text{Eu}^{2+}$  energy transfer is possible because of the overlap between the low-energy absorption band and the emission spectra associated with each one of the precipitated phases.

In a similar way, as in the  $\text{NaCl}:\text{Eu}^{2+}$  system,<sup>12</sup> we can suppose that the transfer between divalent europium ions is of an electric dipole-dipole nature. The expression for this kind of transfer probability is given by

$$P_{dd} = \frac{3\hbar^4 c^4}{4\pi n^4 \tau_S} \left[ \frac{1}{R_{SA}} \right]^6 Q_A \Omega,$$

where  $n$  is the refractive index of the material,  $\tau_S$  is the radiative lifetime of the sensitizer ( $\text{Eu}^{2+}$ ),

$Q_A = \int \sigma_A(E) dE$  is the integrated absorption coefficient for the activator ion ( $\text{Eu}^{2+}$ ),  $R_{SA}$  is the sensitizer-activator ( $\text{Eu-Eu}$ ) distance, and  $\Omega$  is the overlap between the normalized shape  $f_S(E)$  (for the luminescence band of the sensitizer) and the normalized shape  $F_A(E)$  (for the absorption band of the activator):

$$\Omega = \int \frac{f_S(E)F_A(E)}{E^4} dE.$$

In our case,  $f_S(E)$  and  $F_A(E)$  are, respectively, the fluorescence and absorption bands of each type of precipitate. Thus this integral can be evaluated.<sup>16</sup> The values of the overlap integral obtained for each precipitated phase are included in Table I. With these values and the calculation of  $Q_A$  (an averaged value), critical distances [defined as  $P_{dd}(R_C)\tau_S = 1$ ] can also be estimated for each Eu precipitate. The results obtained from these calculations are also included in Table I.

An inspection of this table reveals that, as expected, the higher the critical distance, the smaller the experimental lifetime. Therefore, the model of the quenching of  $\text{Eu}^{2+}$  luminescence induced by europium precipitation provides a very reasonable explanation for the observed experimental data in the high-temperature-annealed sam-

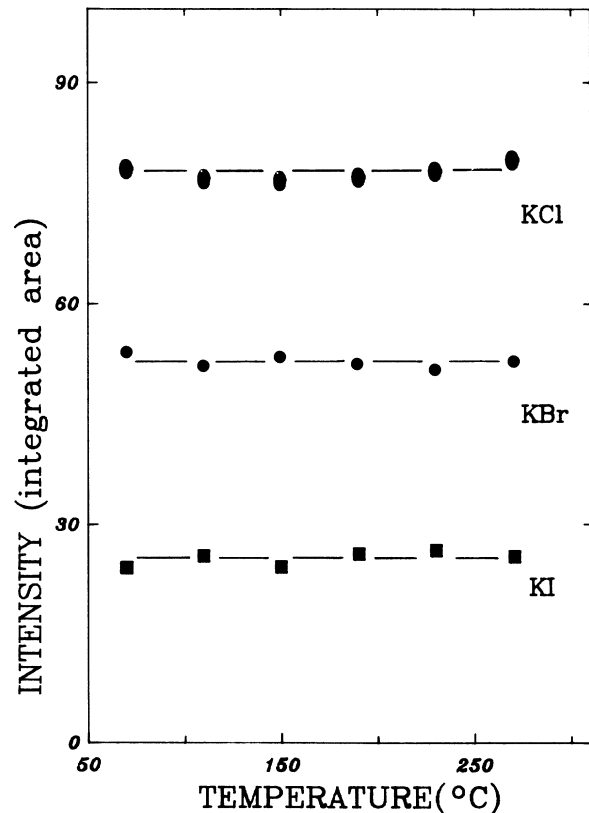


FIG. 5. Emission intensity (area under the curve) as a function of quenching temperature for precipitates formed under annealing at  $T \leq 100^\circ\text{C}$  for the three systems investigated in this work.

ples. If we take these results into account, it is easily inferred that the  $\text{Eu}^{2+}$ - $\text{Eu}^{2+}$  distances, in the  $\text{EuX}_2$  and intermediate precipitates, might be lower than the critical distances calculated in Table I. Unfortunately, there is no direct x-ray experimental evidence on the crystal structure of the dihalide phases nucleated inside potassium halides (or, therefore, the  $\text{Eu}^{2+}$ - $\text{Eu}^{2+}$  distances). In fact, the structure of the  $\text{EuX}_2$  inside the host matrix and that of the natural anhydrous europium dihalides could not be the same. Thus is the case of  $\text{NaCl}:\text{Eu}^{2+}$ , in which x-ray diffraction experiments have shown that  $\text{EuCl}_2$  precipitates have a cubic ( $\text{CaF}_2$ -type) structure,<sup>17</sup> instead of the orthorhombic ( $\text{PbCl}_2$ -type) structure that is typical of the natural form.<sup>18</sup> Anyway, in the cubic structure, the  $\text{Eu}^{2+}$ - $\text{Eu}^{2+}$  distance (4.93 Å) is similar to that obtained in the orthorhombic case (4.48 Å).

In our case, a rough estimation of the  $\text{Eu}^{2+}$ - $\text{Eu}^{2+}$  distances in precipitated phases can be obtained by using the natural anhydrous europium dihalide structures, even though these distances can be changed inside the host matrix. In this respect, the distance between the nearest  $\text{Eu}^{2+}$  neighbors can be estimated as 5.98 Å in  $\text{EuBr}_2$  ( $\text{SrBr}_2$ -type)<sup>19,20</sup> and 5.10 Å in  $\text{EuI}_2$  ( $\text{SrI}_2$ -type).<sup>21</sup> These values are lower than the critical distances calculated in Table II, and therefore energy transfer between europium ions inside stable dihalide phases may be reasonably taking place.

On the other hand, the experimental results reported in this work reveal that precipitation of Suzuki-type phase does not induce quenching of  $\text{Eu}^{2+}$  luminescence and

that the lifetime appears only slightly modified, probably as a consequence of change in the local environment. The absence of quenching in the  $\text{Eu}^{2+}$  luminescence for these kinds of precipitates can now be understood if one takes into account that the  $\text{Eu}^{2+}$ - $\text{Eu}^{2+}$  distance must be larger than the critical distances calculated for these kinds of precipitates, which nucleate at temperatures  $\leq 100^\circ\text{C}$  (which are include in Table II). Therefore, energy transfer between europium ions should not be taking place now. Even though there is no direct x-ray evidence of the presence of  $\text{Eu}^{2+}$  Suzuki phase precipitates in alkali halides, if they are present, the  $\text{Eu}^{2+}$ - $\text{Eu}^{2+}$  distances should be about  $2a$  ( $a$  is the lattice parameter of the host matrix,) giving rise in all cases to higher values than the critical distances reported in Table II.

In conclusion, the strong reduction observed in the  $\text{Eu}^{2+}$  luminescence for the high-temperature-annealed samples ( $T \geq 200^\circ\text{C}$ ) can be attributed to a precipitation-induced quenching as a consequence of the formation of  $\text{EuX}_2$  precipitates. At variance, the annealing of samples at temperatures  $\leq 100^\circ\text{C}$  induces the formation of other types of europium precipitates (probably Suzuki phase), in which the quenching of  $\text{Eu}^{2+}$  luminescence does not occur.

#### ACKNOWLEDGMENTS

This work has been partially supported by the Comisión Interministerial de Ciencia y Tecnología (CI-CYT), Spain.

<sup>1</sup>F. J. López, H. S. Murrieta, J. A. Hernández, and J. O. Rubio, *Phys. Rev. B* **22**, 6428 (1980).  
<sup>2</sup>J. O. Rubio, H. S. Murrieta, J. A. Hernández, and F. J. López, *Phys. Rev. B* **24**, 4847 (1981).  
<sup>3</sup>F. J. López, H. S. Murrieta, J. A. Hernández, and J. O. Rubio, *J. Lumin.* **26**, 129 (1981).  
<sup>4</sup>M. Aguliar, J. O. Rubio, F. J. López, J. García Solé, and H. S. Murrieta, *Solid State Commun.* **44**, 141 (1982).  
<sup>5</sup>C. Medrano, H. S. Murrieta, and J. O. Rubio, *J. Lumin.* **29**, 223 (1984).  
<sup>6</sup>F. Cussó, J. García Solé, H. S. Murrieta, J. O. Rubio, and F. J. López, *Cryst. Lattice Defects Amorph. Mater.* **10**, 99 (1982).  
<sup>7</sup>J. E. Muñoz Santiuste, F. Jaque, J. García Solé, and P. Aceituno, *Cryst. Lattice Defects Amorph. Mater.* **16**, 246 (1987).  
<sup>8</sup>R. Capelletti and M. Manfredi, *Phys. Status Solidi A* **86**, 333 (1984).  
<sup>9</sup>H. Opyrchal and M. Manfredi, *Phys. Status Solidi A* **103**, 93 (1987).  
<sup>10</sup>E. Mugensky and R. Cywinsky, *Phys. Status Solidi B* **125**, 381 (1984).  
<sup>11</sup>D. Cassi, M. Manfredi and M. Solzi, *Phys. Status Solidi B* **135**, K143 (1986).

<sup>12</sup>J. E. Muñoz Santiuste and J. García Solé, *Phys. Rev. B* **38**, 10874 (1988).  
<sup>13</sup>I. Aguirre de Carcer, F. Cussó, and F. Jaque, *Phys. Rev. B* **38**, 10 812 (1988).  
<sup>14</sup>C. Zaldo, J. M. Calleja, and E. M. Orozco, *J. Phys. C* **220**, 849 (1987).  
<sup>15</sup>C. Zaldo, E. M. Orozco, A. A. Mendoza, and J. O. Rubio, *J. Phys. D* **18**, 247 (1985).  
<sup>16</sup>Because of strong overlapping, the absorption bands of the different types of precipitates cannot be separated in the overall absorption spectrum. Consequently, the same low-energy absorption band (an average of the three types of precipitates, intermediate and final stable dihalide phases) was used for each.  
<sup>17</sup>J. Stepien-Damm and K. Lukaszewicz, *Acta Crystallogr. A* **36**, 54 (1980).  
<sup>18</sup>H. Bärnighausen, *Rev. Chim. Miner.* **10**, 77 (1973).  
<sup>19</sup>J. M. Haschke and H. A. Eick, *J. Inorg. Nucl. Chem.* **32**, 2153 (1970).  
<sup>20</sup>J. G. Smeggil and H. A. Eick, *Inorg. Chem.* **10**, 1449 (1971).  
<sup>21</sup>E. Th. Rietschel and H. Bärnighausen, *Z. Anorg. Allg. Chem.* **368**, 62 (1969).